Reprinted from

STRENGTH OF METALS AND ALLOYS

(ICSMA 8)

Proceedings of the 8th International Conference
on the Strength of Metals and Alloys
Tampere, Finland, 22–26 August 1988

Edited by
P. O. KETTUNEN, T. K. LEPISTÖ,
M. E. LEHTONEN

PERGAMON PRESS
OXFORD · NEW YORK · BEIJING · FRANKFURT
SÃO PAULO · SYDNEY · TOKYO · TORONTO

Deformation Characteristics and Work-hardening Behaviour of some High Strength Manganese Steels

A. O. Inegbenebor, R. D. Jones and Brian Ralph*

Institute of Materials, University College, Cardiff, UK
**Now at Department of Materials Technology, Brunel, the University of West London, Uxbridge, Middlesex, UK*

ABSTRACT

A study has been made on a new type of wear resistant/high strength iron-manganse-molybdenum steel. This study includes the influence of composition and heat treatment on the mechanical properties. The exceptional work-hardening rate is due to strain-induced formation of lath martensite which itself also takes part in the work-hardening process. The influence of higher molybdenum contents was evident in preventing brittleness of the solution treated steels. An optimum composition range for this type of steel is indicated.

KEY WORDS

Wear resistant steel, high strength iron-manganese-molybdenum steels, unstable austenite/epsilon martensite, maraging steels, Hadfield manganese steel, magnetic reluctance technique, strain-induced lath martensite, exceptional work-hardening.

INTRODUCTION

This new wear resistant/high strength iron-manganese-molybdenum steel was originally intended as a lower cost maraging material (Jones and coworkers, 1982). It was observed that this steel work-hardens very rapidly in the early stage of deformation and simultaneously possesses higher strength than Hadfield manganese steel.

Hadfield manganese type steels (composition around 14% Mn, 1% C), do not transform to lath martensite (White and Honeycombe, 1962), but work-harden very considerably through interaction of stacking faults with interstitials (carbon) and formation of epsilon martensite. There can be problems in welding Hadfield manganese steels, however, in this new wear-

resistant iron-manganese-molybdenum steel weldability is safeguarded by the low carbon content and costs are reduced since it can be used in the hot-rolled condition. The alloys in the present study were expected to combine solid solution strengthening effects with the work-hardening caused by an increased dislocation density and stacking fault population which are generated in the austenite/epsilon martensite matrix during the strain-induced formation of lath martensite.

MATERIALS AND EXPERIMENTAL METHODS

During the course of the investigation, a large number of experimental low carbon steels have been produced but this paper is limited to a consideration of only a few of the alloys. All tensile tests were carried out at a constant cross-head speed (0.5mm/min.) corresponding to an initial strain rate of $8.33 \times 10^{-3} s^{-1}$. The phase content of the steels was determined using a commercial "Ferritescope" which quantified ferromagnetic phase contents by monitoring magnetic reluctance in-situ.

RESULTS

The volume fraction of lath-martensite in the higher manganese alloys which transformed was found to increase as the plastic strain increased (fig. 1) which can be compared with the results of other workers (e.g. Olson and Cohen, 1972 and Hecker and coworkers, 1982)).

Examples of the true stress/true plastic strain curves of some of the higher manganese alloys and tensile work-hardening rate/true plastic strain curves obtained at early stage of deformation are given in figs. 2 and 3. The overall flow stress levels and trends of the curves show how, as the transformation progressed the work-hardening of the steels increased rapidly. This phenomenon has resulted in the impressive mechanical properties of both hot-rolled and solution treated samples which are given in the table. Figure 4 shows the experimental curves and curve calculated from the model. It may be seen from the curves that the experimental and model curves are very close.

Table. Mechanical Properties

Alloy	Elastic Limit [MPa]	0.2% P.S [MPa]	T.S. [MPa]	Elong. %	Red.in area %	"n"
Fe-11Mn-4Mo*	333	364	1470	18	54	0.550
Fe-12Mn-3Mo*	415	455	1276	20	25	0.643
Fe-13Mn-3Mo*	234	256	1392	18	10	0.447
Fe- 9Mn-2Mo**	500	549	882	16	65	0.319
Fe-11Mn-4Mo**	312	338	1436	18	60	0.512
Fe-12Mn-3Mo**	393	432	1304	19	45	0.580
Fe-13Mn-3Mo**	212	230	1172	10	7	0.410

*Hot-rolled condition ** Sol. treated 950 ℃ for 1 hour

MODEL OF PROCESS

The high strength of these multiphase steels can be explained by a mechanism of composite strengthening assuming a modification of the law of mixtures to be valid. In this model the composite flow stress has been derived and combined with the constitutive flow relation for a metastable austenitic steel during strain-induced martensitic transformation developed by Narutani, Olson and Cohen (1982).

Suppose:-

$$\sigma c = V^{\circ}_{\alpha'}\ \sigma_{\alpha'} + V^{\circ}_{\gamma+\varepsilon}\ \sigma_{\gamma+\varepsilon} \qquad [1]$$

$$\varepsilon c = V^{\circ}_{\alpha'}\varepsilon_{\alpha'} + V^{\circ}_{\gamma+\varepsilon}\ \varepsilon_{\gamma+\varepsilon} \qquad [2]$$

Where V°_{α} and $V^{\circ}_{\gamma+\varepsilon}$ are the initial volume fraction of the lath martensite and austenite/epsilon martensite respectively, $\sigma_{\alpha'}$, $\varepsilon_{\alpha'}$ and $\sigma_{\gamma+\varepsilon}$, $\varepsilon_{\gamma+\varepsilon}$ are the corresponding true stresses and strains of austenite/epsilon martensite and εc are the composite flow stresses and strains.

From Inegbenebor, Jones and Ralph (1987), a modified Ludwik-Holloman equation may be written:

$$\sigma_{\gamma+\varepsilon} = K[\ln(1+e)]^{n}\ V^{\circ}_{A+\varepsilon}\left[1-\left(1+\frac{e}{A}^{-S}\right)^{-1}\right] \qquad [3]$$

where $\sigma_{\gamma+\varepsilon}$ represents the ease with which an austenite/epsilon structure can undergo a strain-induced transformation to lath martensite, K is the austenite/epsilon martensite strengthening factor, e, is engineering strain, n, is the work-hardening factor, A, is a proportionality constant and S, is the automotive lath martensite index.

Also from Inegbenebor (1988), it has been shown

$$\sigma_{\alpha'} = T\left[V^{\circ}_{\alpha'} + V^{\circ}_{\gamma+\varepsilon}\left(1+\frac{e}{A}^{-S}\right)^{-P}\right] \qquad [4]$$

where T is lath martensite strengthening factor and P is the lath martensite index.

If the expression for $\sigma_{\gamma+\varepsilon}$ and $\sigma_{\alpha'}$ in equations [3] and [4] respectively are substituted into equation [1] the following expression arises:

$$\sigma c = V^{\circ}_{\gamma+\varepsilon}\ K[\ln(1+e)]^{n}\ V^{\circ}_{\gamma+\varepsilon}\left[1-\left(1+\frac{e}{A}^{-S}\right)^{-1}\right]+V^{\circ}_{\alpha}$$
$$T\left[V^{\circ}_{\alpha}+V^{\circ}_{\gamma+\varepsilon}\left(1+\frac{e}{A}^{-S}\right)^{-P}\right]$$

This flow-curve equation can be combined with the model developed by Narutani, Olson and Cohen (1982) which is:

$$\sigma\{[1 - f] \cdot \sigma_{\gamma}(\varepsilon - \alpha f) + f \cdot \sigma_{\alpha'}(\varepsilon - \alpha f)\}\left[1 - B \cdot \frac{df}{d\varepsilon}\right]$$

[Here, $\alpha = 0.12$, f is the volume fraction of lath martensite, ε is the plastic strain and $\beta = 5.3 \times 10^{-2}$].

By a combination of the two composite flow stresses, the following expression arises:

$$\sigma = \{[1 - f) \cdot K[\ln(1 + e)]^{n} V^{\circ}_{\alpha+\varepsilon}[1 - (1 + \frac{e^{-s}}{A})^{-1}] [\varepsilon - \alpha f] +$$

$$T[V^{\circ}_{\alpha} + V^{\circ}_{\gamma+\varepsilon}(1 + \frac{e^{-s}}{A})^{-P}] [\varepsilon - \alpha f]\} \cdot [1 - \beta \cdot \frac{df}{d\varepsilon}]$$

DISCUSSION

The irregular nature of the curves in fig. 1 seems to suggest a transformation 'burst' phenomenon (Guimaraes (1987)) during plastic deformation. This might be associated with the "brickwork" martensitic structure which forms in these steels as a result of the fragmentation of the original austenite on $(111)_{\gamma}$ planes by thin layers of epsilon phase. This is an intermediate in the transformation to lath martensite as the structure undergoes strain-induced transformation as reported by Bogachev and coworkers (1975) and Jones and coworkers (1982). What happens is that the nucleation of one lath triggers off the formation of another lath in an adjacent region as plastic strain increases. In the model of Olson and Cohen (1975), the formation of martensite by plastic deformation and how this is affected by stacking fault energy and strain rate has been explained. During strain-induced transformation, plastic deformation of the parent phase creates the correct defect structures to act as embryos for the transformation products. This will result in a higher dislocation density in the end product and increased stacking fault population in the austenite/epsilon matrix. Therefore, the rapid work-hardening in the low strain region of these alloys is due to strain-induced formation of fine, heavily dislocated lath martensite and also probably to an increase in stacking faults in austenite as a result of the strain-induced transformation. The calculated curve from the model as compared with the experimental curve in figure 4, demonstrates excellent agreement.

Figures 5 and 6 show the ductile and intergranular failure are shown of alloys which have been solution treated at 1150 C. The influence of a higher molybdenum content in preventing brittleness can be observed. From the mechanical properties of a large number of experimental steels we have established the ideal composition range for wear resistance application such as for railway points and crossings as:

11-12.5% Mn, 2-4% Mo, 0.2% C max., 0.4% Si max., 0.02% S max., 0.03% P max., balance Fe. This range covers air and vacuum melts.

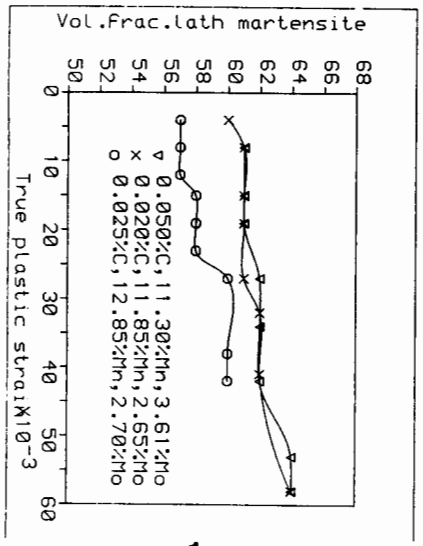

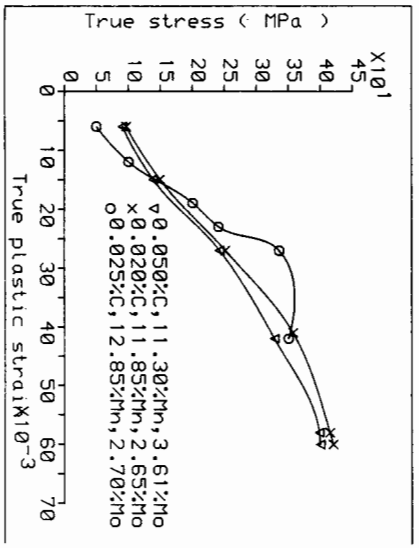

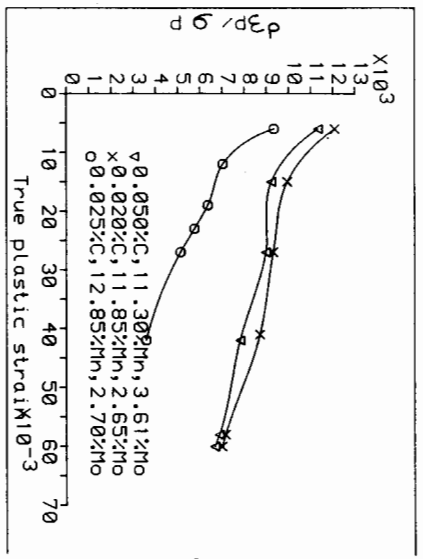

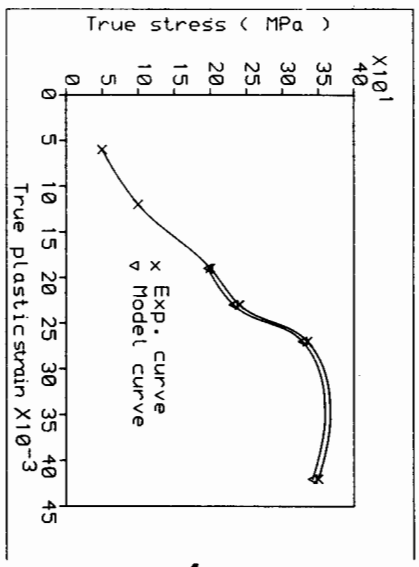

Fig. 1 Volume fraction of lath martensite vs. true plastic strain

Figs 2-3 Tensile true-stress and work-hardening rate vs. true plastic strain, s.t. at 950°C for 1 hr.

Fig. 4 Curve fitting of the theoretical model (0.025% C, 12.85% Mn, 2.7% Mo) at 950°C for 1 hr.

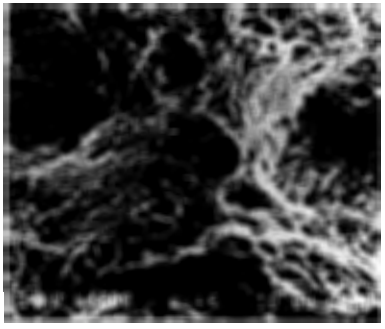

5

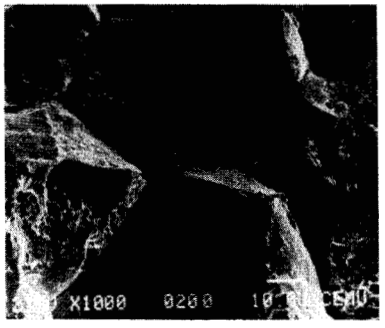

6

Fig. 5 Fracture surfaces (SEM) of (0.05% C, 11.30% Mn, 3.61% Mo) s.t. at 950°C for 1 hr.

Fig. 6 Fracture surfaces (SEM) of (0.025% C, 12.85% Mn, 2.70% Mo) s.t. at 1150°C for 1 hr.

REFERENCES

Bogachev, I.N., Khadayev, M.S. and Nemirovskii, Yu.R. (1975). Martensitic Transformations in Fe-Mn Alloys. Phys Met Metallogr., 40, (4), 69-77.

Guimaraes, J.R.C., (1987). Initial Nucleation Sites, Autocatalysis and the Spread of the Martensite Burst in Fe-31.9Ni-0.02C. Mat. Sci. and Eng., 95, 217-224.

Hecker, S.S., Stout, M.G., Staudhammer, K.P. and Smith, J.L. (1982). Effects of Strain State and Strain Rate on Deformation-induced Transformation in 304 Stainless Steel, Magnetic Measurements and Mechanical Behaviour. Met. Trans., 13A, 619-626.

Inegbenebor, A.O., Jones, R.D. and Ralph, B. (1987). Models of Tensile Behaviour of Meta-stable Fe-Mn-Mo Alloys. In proc. of 8th Riso Int. Symp. on constitutive relations and their physical basis, p.345-352.

Inegbenebor, A.O. (1988). Ph.D thesis, University of Wales.

Jones, R.D., Palmer, G.R., Jerath, V., Kapoor, S. and Yeldham, R. J. (1982). The Development of a High Strength Manganese Steel. In Proc. of 6th ICSMA, 1225-1230.

Narutani, T., Olson, G.B. and Cohen, M. (1982). Constitutive Flow Relations for Austenitic Steels During Strain-induced Martensitic Transformation. J. de Phys., 43, C4-429.

Olson, G.B. and Cohen, M. (1972). A mechanism for the strain-induced Nucleation of Martensitic transformations. J. Less-Com. Met., 28, 107-118.

Olson, G.B. and Cohen, M. (1975). Kinetics of Strain-induced Martensitic Nucleation. Met. Trans., 6A, 791-795.

White, C.H. and Honeycombe, R.W.K. (1962). Structural Changes during the Deformation of High Purity Iron-Manganese-Carbon Alloys. J. Iron and Steel Inst., 200, 457-466.